REVISTA MATÉRIA V.29 N.4
ISSN 1517-7076 articles e20240517, 2024

Characterization of mandacaru (*Cereus jamacaru DC.*) and its use in lightweight bio-concrete

Mariana Nayara Lima Silveira[1], Luisa de Oliveira Menali[1], Uasmim Lira Zidanes[2], Matheus Cordazzo Dias[3], Jenaina Ribeiro Soares[4], M'hamed Yassin da Gloria[5], Fábio Akira Mori[2], Eduardus Koenders[6], Romildo Dias Toledo Filho[5], Saulo Rocha Ferreira[1]

[1]Universidade Federal de Lavras, Departamento de Engenharia Civil. 3037, 3720-900, Lavras, MG, Brasil.

[2]Universidade Federal de Lavras, Departamento de Ciências Florestais. 3037, 37200-900, Lavras, MG, Brasil.

[3]Universidade Estadual do Amapá, Departamento de Engenharia Florestal. Av. Presidente Vargas, 650, Central, 68900-070, Macapá, AP, Brasil.

[4]Universidade Federal de Lavras, Departamento de Física. 3037, 37200-900, Lavras, MG, Brasil.

[5]Universidade Federal do Rio de Janeiro, Departamento de Engenharia Civil. 68506, Rio de Janeiro, RJ, Brasil.

[6]Technische Universität Darmstadt, Institut für Werkstoffe im Bauwesen. Darmstadt, Germany.

e-mail: uasmimzidanes@hotmail.com, mariana.nalisi@gmail.com, luisamenaali@hotmail.com, matheus.cordasso@gmail.com, jenaina.soares@ufla.br, ydagloria@yahoo.fr, morif@ufla.br, koenders@wib.tu-darmstadt.de, toledo@coc.ufrj.br, ferreira.sr@hotmail.com

ABSTRACT

The Cactaceae family is a suitable alternative for future sustainable development in the construction industry. In addition to being a renewable raw material, these plants grow with ease and are extremely adaptable to the most diverse and rigorous climates and poor soil. The *Cereus jamacaru* DC. has a woody structure that is unknown and, consequently, unexplored. This research aimed to characterize the secondary xylem of cactus and to evaluate its use in the development and characterization of lightweight bio-concrete. The anatomical properties were used characterized. The chemical composition, crystallographic structure thermogravimetric analysis was evaluated. To produce bio-concrete, the wood was washed in hot water, and flow table and uniaxial compression tests were performed. The results indicate that the species has a high extractive content and a low density. The bio-concretes produced are lightweight and show promising results for the use of *C. jamacaru* wood in the construction industry. The combination of bioconcrete, with its sustainable properties, and lignocellulosic reinforcements, which provide greater strength and lightness, results in a material with unique and advantageous characteristics. Possible applications include non-structural elements such as walls, cladding and partitions. And in low-load structural elements such as slabs and pillars.

Keywords: Cactus wood; Renewable materials; Bioaggregates; Lightweight Bio-concrete.

1. INTRODUCTION

The vast growth of the world population has generated massive environmental problems, leading to a sustained exhaustion of the natural resources of our planet. The current civil construction sector has a demand for natural resources and generates amounts of construction and demolition waste. From a sustainability perspective, there is a strong need to develop new technologies and materials that meet the present environmental and durability demands [1–3].

To develop composite materials, many studies have already been carried out on both cementitious matrices and lignocellulosic components, which have shown enhanced durability, strength and ductility [4–6]. There are various environmental benefits of using lignocellulosic biomass, including sustainability and low energy consumption. Another advantage of such natural resources is related to the ability to use them as bioaggregates in lightweight concretes [2].

Wood particle wastes are very often used for bio-concrete production. However, there are several other lignocellulosic materials with a similar or higher potential for use in such applications. The species Cereus jamacaru, popularly known as mandacaru, is native to Caatinga (tropical dry forest) and is one of the most uncommon and understudied Brazilian biome plant products [7]. The origin is from the *Cactaceae* family, are an

Corresponding Author: Uasmim Lira Zidanes Received on 06/08/2024 Accepted on 08/11/2024

DOI: https://doi.org/10.1590/1517-7076-RMAT-2024-0517

(cc) BY

innovative source of biomass. They are environmentally friendly because of their renewability and recyclability. They also have highly competitive potential in the current market since they are extremely adaptable to most harsh habitats, growing easily in regions with infertile soils, and can withstand high temperatures and/or low humidities [7–9].

In recent decades, *C. jamacaru* has attracted increasing attention, especially due to its economic, medicinal and industrial prospects related to the production of wax esters, which could be used as impermeable barriers, alkaloids, as ingredients in cosmetic and pharmaceutical formulations and in food sciences [10–15]. The cactus mucilage can be used as an additive to plaster, cement, and lime-based mortars. Studies indicate that it was used in old buildings in Brazil and Mexico [16–18].

In this study, *C. jamacaru* wood was characterized, and its use in the production of wood-based bio-concrete was evaluated. This type of cactus wood exhibits peculiar characteristics when compared to common woods, and these characteristics could explain its adaptation to natural and harsh environments.

2. MATERIALS AND METHODS

2.1. Materials

The wood of *C. jamacaru* was obtained from a commercial plantation in Barueri - SP, Brazil and was extracted from the base of a three-year-old plant by manual cutting. Small sections were prepared and used for physical, chemical, and morphological analysis. Detailed properties of the wood are reported in the following subsections.

2.2. Anatomical planes of wood by light microscopy

Histological slides were prepared from the permanent wood of *C. jamacaru* and used for the microscopic analysis of the anatomical planes. The specimens were saturated by immersion in water and sectioned in a slide microtome, which was set at 15 μm thickness. From the histological sections of *C. jamacaru*, the secondary xylem was discolored, dehydrated, and recolored with safranin 1%.

Afterward, the cuts were mounted on slides and cover slips and fixed in Entellan. Approximately ten permanent slides were taken from three specimens of separate places on the shaft, with a diameter, width, and thickness of 2 × 2 × 2 cm, respectively. To accomplish the necessary measurements, quantitative analysis was performed with ImageJ, a free Java-based software.

2.3. Scanning Electron Microscopy – SEM of cactus wood

First, the specimens measuring 2.5 × 2.5 × 2.5 cm were prepared and placed in a container with water to saturate them and facilitate microtome cutting. After saturation, the cactus wood specimens were cut into 15 μm thick slices while retaining the surfaces of interest. The cuts were performed to make the surfaces of the various specimens smooth and clean for better visualization of the wood microstructure. After that, new specimens with dimensions of approximately 0.5 × 0.5 × 0.5 cm were prepared from the original specimens, preserving the surfaces where the histological sections were made. Finally, the samples were oven dried with air circulation at a temperature of 40°C for 24 hours. A thin layer of gold was applied to make the specimens conductive and appropriate for study. The specimens were fixed in a metal stub covered by carbon-coated tape. The anatomical structure of wood was evaluated employing an SEM LEO EVO 40 (Carl Zeiss, Germany) scanning electron microscope. The device was operated under an accelerating voltage of 20 kV.

2.4. Morphological characterization by light microscopy

Quantitative morphological and anatomical characterization of the wood and its fibers was performed following the method proposed by IAWA [19] and FRANKLIN [20]. For the anatomical description, the IAWA standard, which defines all major elements that need to be characterized and identified, was used. For the fiber studies, acetic acid and hydrogen peroxide were applied in a 1:1 ratio, thus facilitating the dissociation of fibrous elements. The images were processed with ImageJ. An CX31light microscope (Olympus, Japan) and BEL capture system were used. Images were obtained with a 4x and 40x magnification lens.

From the generated images with an objective lens and a 4x amplification, it was possible to measure the fiber length, and with the 40x amplification, it was possible to measure the diameter and lumen thicknesses of the fibers. The cell wall thickness was obtained by Equation 1:

$$\mathrm{CWT} = \frac{(D - LT)}{2} \tag{1}$$

where CWT is the cell wall thickness, D is the diameter of the fibers and LT is the lumen thickness. The relation between compressive strength, density and cellulose content was calculated by the stiffness coefficient according to Equation 2:

$$SC = \frac{2\,CWT}{D} \tag{2}$$

where *SC* is the stiffness coefficient, CWT is the cell wall thickness *D* and is the diameter of the fiber. From this equation, SC values of 0.45 were found, which represent cell walls that can be classified as medium thickness [19–22].

It is also possible to calculate the spin index λ of *C. jamacaru* fibers from Equation 3 below:

$$\lambda = \frac{L}{D} \tag{3}$$

where L is the fiber length and *D* the fiber diameter. The closer the diameter is to the fiber length, i.e., $\lambda \approx 1$, the larger the mechanical stability for a given application loaded in the fiber direction. The average index found was 23.17, and this was a good result compared to values obtained in other characterizations, indices found in other studies include 78.8 [23], 36.66 [24] and 65.26 [25].

2.5. Chemical characterization

The cactus wood was ground and sieved to generate particles with lengths ranging between 0.25 and 0.40 mm. The total extractives were quantified from an adaptation of the standard TAPPI T204 cm-17. Acetone extraction was performed with a Soxhlet extractor for five hours, followed by a final wash with hot water at 80°C. The TAPPI T211 om-16 procedure was applied to determine the content of the necessary ash. The materials were heated to 525°C in a muffle furnace, where they remained at this temperature for three hours. The insoluble lignin was quantified according to standard TAPPI T222 om-15 by the hydrolysis method. The holocellulose content was obtained following the procedure described in a prior report [26]. The suspension was stirred at room temperature for 15 h and then filtered. The solid residue (cellulose) was washed with water to neutralize the filtrate with two portions of 1% acetic acid, and it was finally washed with ethanol. Then, starting from dry holocellulose, the cellulose content and hemicellulose were determined following a procedure described previously [27].

2.6. Thermogravimetric analysis (TGA)

Particles of cactus wood with a maximum size of 74 μm were subjected to heating. The thermogravimetric analyses were performed on an STA 449 F5 Jupiter instrument from NETZSCH. The particles were heated from 25°C to 1000°C under nitrogen atmosphere with a heating rate of 10°C/min. Open alumina crucibles were used in the tests.

2.7. FT-IR spectroscopy-Attenuated Total Reflectance (ATR)

The analysis was performed using cactus wood particles, employing an FTIR Spectrometer Varian 600-IR Series equipped with a GladiATR from Pike Technologies. The samples were scanned from 4000 to 400 cm^{-1} with 32 scans at a resolution of 4 cm^{-1}.

2.8. X-Ray Powder Diffraction (XRD) analysis

Crystallographic patterns were evaluated with an X-ray diffractometer (Bruker D2 Phase 2nd Generation) with a Cu-Kα source (λ = 1.54184 Å), 30 kV, in the 2θ range of 10-40 at a scan rate of 0.5°/min and an increment of 0.02° 2θ. The detector was a Lynxeye (1D mode).

The theoretical coordinates of cellulose II were extracted from the crystallography data (.cif) using Mercury 2020.2.0 software (CCDC, UK) obtained from the Supplementary Information accompanying the original work [28].

The patterns were deconvoluted using the Gaussian function with Magic Plot 2.9 (Magicplot Systems, Russia). For the amorphous halo, the cellulose II pattern with full width at half maximum (FWHM = 9), only varying its intensity, was used, as suggested in the literature [29]. After deconvolution, the crystalline fraction (CF) was calculated from the ratio between the area below all the crystalline peaks and the total area below the curve, determined after deconvolution from Equation 4:

$$CF(\%) = \frac{\sum \text{Area}_{\text{Crystalline Peaks}}}{\sum \text{Area}_{\text{Crystalline Peaks}} + \text{Area}_{\text{Amorphous Halo}}} \times 100 \quad (4)$$

where $A_{(crys)}$ is the area of the theoretical crystalline fraction, and $I_{(am)}$ is the area of the theoretical amorphous fraction of cellulose. For comparison, Segal's crystalline index was calculated according to the Segal method [30], which is based on the height of the amorphous material and the total intensity.

The crystallite size of a sample was calculated using Scherrer's equation (Equation 5) [31]:

$$\tau = \frac{K\lambda}{\beta \cos \theta} \quad (5)$$

where τ is the size perpendicular to the lattice plane represented by the peak regarding the plane (200), K is a constant that depends on the crystal shape, λ is the wavelength of the incident beam in the diffraction experiment, β is the FWHM in radians and is the position of the peak in radians. This step was conducted using theoretical curves.

2.9. Raman spectroscopy

Prior to the Raman spectroscopy measurements, samples of the wood were macerated by the method described in an earlier report [20] and stored in a bath of ethanol. These samples were measured by using a 532 nm excitation laser (green) with a LabRAM HR Evolution spectrometer from Horiba Scientific-Japan, which had an objective lens of 50x. The measurements were performed at 25% of the nominal laser power of 100 mW to avoid sample heating and degradation in a range from 4000 to 250 cm^{-1}.

The data were submitted to a background correction performed according to a procedure described by other researchers [32, 33]. This procedure is based on subtracting the fluorescence and excluding the baseline by a fourth-order polynomial fit. To minimize systematic variations, the Raman spectra were normalized to a unit vector.

From the normalized intensity of the Raman spectra, it was possible to estimate the crystallinity of the cellulose of the cactus fibers by Equation 6, described in a prior study [32]:

$$X_{\text{Raman}} = \frac{(I_{380} \div I_{1096}) - 0.0286}{0.0065} \quad (6)$$

where I_{380} and I_{1096} are the intensities for the 380 and 1096 cm^{-1} Raman active bands.

2.10. Mechanical characterization by axial compressive strength test

Compressive strength tests on specimens with dimensions of 10 × 10 × 20 mm (width × height × length) were performed on an electromechanical testing machine developed by Kammrath Weiss GmbH. Five wood samples were evaluated using a load cell of 5 kN and a displacement rate of 0.1 mm/min. The dimensions of the specimens were selected based on standard DIN 52185–78, which recommends specimen sizes of 30 × 30 × 60 mm. From this, the size was reduced to specimens containing small representative pieces of cactus wood.

The literature confirms the possibility of performing mechanical evaluation tests on small or microsized specimens. The probability of defects occurring in a solid is proportional to its size, and consequently, the mechanical resistance is statistically higher in small specimens [34–36].

The influence of the size of the specimens, the so-called size effect, has also been reported by other researchers. The compressive strength of the microsized samples (3 mm × 3 mm × 5 mm) was only 2.6% lower than that of the standard-sized samples (20 mm × 20 mm × 30 mm). Based on this information, microsized test samples are considered appropriate for estimating the standard-size results in experiments where the size effect was neglected. Similar results were also obtained in [34–36].

2.11. Physical characterization: basic density and water absorption

To determine the basic density of wood and its water absorption capacity, a procedure following the standard ASTM D2395–17 [37] was adopted. Based on this standard, small sections of mandacaru were left submerged in water until they reached the point of saturation, and after that, both their mass and the volume were measured. After 72 hours in the oven at 103 ± 2°C, their dry and stable masses were measured again.

2.12. Lightweight bio-concrete production

2.12.1. Bioaggregate

To produce bio-concrete, bioaggregates (Figure 1a) were crushed in a hammer mill, and particles with a length of 0.5 to 10 mm were created (Figure 1b). A washing cycle experiment based on the work of ANDREOLA *et al*. [38] was performed to determine the number of washing cycles required to reduce the extractives from the bioaggregate particles (Figure 1c).

As a result, the particles were washed eight times in hot distilled water. A ratio of 1 g/60 ml was used between particle mass and water volume and was heated to 80°C for one hour. After each washing cycle, the particles were separated from the water, washed again, and prepared to start for another cycle.

A continuing change in the water colour (Figure 1c) was observed, this variation can be explained by the removal of extractives from the material. It can be noted that this removal of extractives occurred during the first three washing cycles, since there is not significant difference in coloration from the third to the last. Thus, it was concluded that 3 washing cycles is sufficient to production of bio-concrete. However, the lesser amounts of lignin remaining in the bioaggregates after three washing cycles still affected the start of the hydration process (stretching the dormant stage).

The apparent density of bioaggregate particles was characterized according to standard ASTM D2395-17 [37]. The result was 0.25 ± 0.05 g/cm^3.

2.12.2. Binder and additives

Previous work on wood cement composites [39, 40] obtained satisfactory results using Brazilian CPV-ARI Portland cement as the binder. The chemical composition and density of the cement are provided in Table 1. Moreover, 3% calcium chloride ($CaCl_2$), based on the cement mass, was used to accelerate cement hydration.

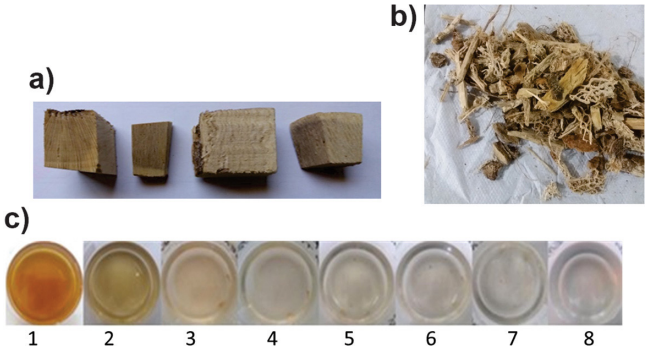


Figure 1: (a) Raw commercial cactus wood, (b) cactus wood particles, (c) water of wood particles after 8 washings cycles.

Table 1: Chemical composition and density of cement CP V - ARI.

CHEMICAL COMPOSITION	PERCENTAGE (%)
CaO	70.140
SiO_2	15.475
Al_2O_3	4.870
SO_3	4.207
Fe_2O_3	3.458
K_2O	1.028
SrO	0.407
TiO_2	0.244
MnO	0.138
CuO	0.016
ZnO	0.015
Density	3.17 g/cm^3
Specific surface area	470 m^2/g

Table 2: Mix design.

BLEND	WOOD VOLUME (%)	MASS RATIO					
		CEMENT	WOOD	W/C	COMPENSATION WATER	W/C EFFECTIVE	$CaCl_2$
CBC100	45.0	1	0.145	0.4	0.145	0.545	0.03
CBC200	45.0	1	0.145	0.4	0.290	0.690	0.03

2.12.3. Bio-concrete production

Table 2 shows the mix design used to produce the two-cactus bio-concretes (CBCs). The cement mass and the volume of wood were chosen according to a prior study [38], and for all mixtures, the water-to-cement ratio (w/c) was 0.4.

The high water absorption of bioaggregates was explicitly considered to keep the fibers saturated to allow proper cement hydration and to adhere to the predefined consistency of the bio-concrete [40]. Thus, additional water was added to the mixture to compensate for this absorption. For CBC100, 100% compensation water (relative to wood mass) was added, and 200% was added to CBC200. The latter addition of water was performed to compensate for both the absorption of the bioaggregates and the loss of workability caused by the bioaggregates. However, this addition also affected the water:cement ratio, leading to the so-called "effective water/cement ratio." These data are also provided in Table 2.

The CBC mixtures were produced in a 5-liter planetary mixer. The calcium chloride capsules were dissolved in mixing water (which included the compensation water) in a reserved container, forming a homogeneous solution. Then, the cement and wood bioaggregates were added to the mixer and homogenized for 1 min. Next, water was gradually added to the dry materials for one more minute, but this addition was interrupted so that the material attached to the bottom and surfaces of the mixer could be manually detached. The mixing continued for 5 minutes in total.

5 × 10 cm cylindrical specimens of were manufactured. The molds were filled in three layers, while compaction was performed manually with 15 strokes per layer according to the ASTM C39/C39 M-18 [41] standard. The specimens were protected against moisture loss with plastic foil until demolding, which was performed after one day. After all, the specimens were positioned in a climate chamber at 20 ± 2°C and 95 ± 2% RH until they reached 28 days of age.

In the fresh state, for each mixture, consistency was evaluated using the flow table test by averaging the two perpendicular diameters of the spread. Based on ASTM C39/C39M-18 [41], the compressive test was performed after 28 days on a Shimadzu-1000 kN universal testing machine at a rate of 0.3 mm/min.

The vertical displacement was obtained by averaging the two linear variable differential transformers (LVDTs). For each mixture, four specimens were evaluated. The ASTM C469/C469M-14 [41] standard was used for determination of the modulus of elasticity.

3. RESULTS AND DISCUSSION

3.1. Physical properties

The values for density and water absorption of the wood are shown in Table 3.

According to the classification of the ASTM D2395-17 standard, the wood of *C. jamacaru* can be classified as low density. The measured densities are consistent and reflect the high internal porosity of the material.

3.2. Morphological characterization

With the analysis of the three different cuts of the secondary xylem, i.e., transversal, radial and tangential (Figure 2), it was possible to identify the microscopic characteristics of the wood. The growth rings representing the inner microstructural boundaries are clearly visible. Uniform diffuse porosity, multiple vessels were present and mostly in lumped into configurations of 2 or 3, but solitary vessels were also observed (Figure 3a).

Table 3: Physical properties of the *C. jamacaru* cactus wood.

WATER ABSORPTION (%)	BASIC DENSITY (g/cm^3)
199 ± 11	0.34 ± 0.1

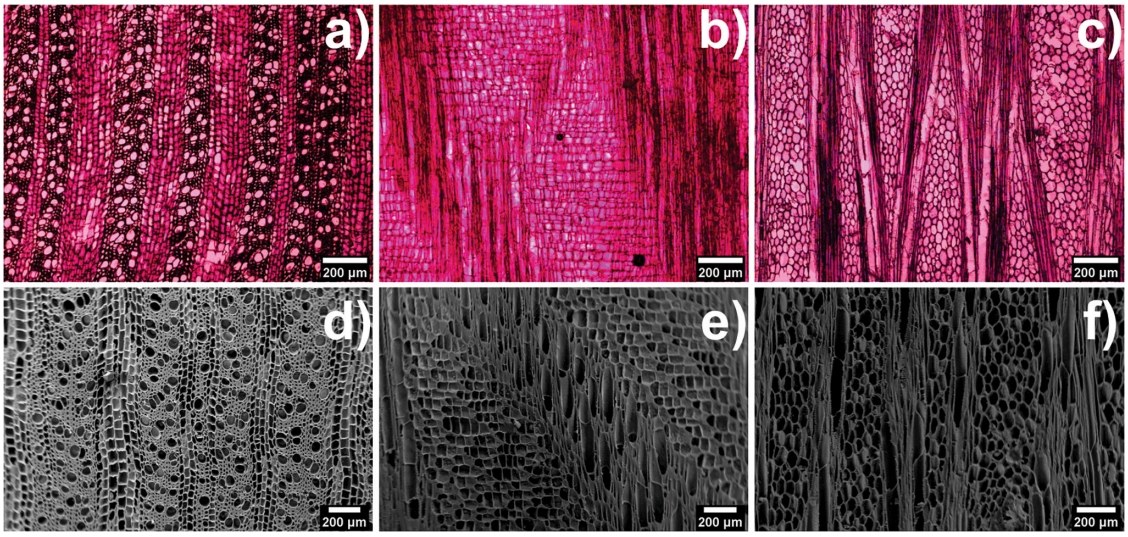


Figure 2: *C. jamacaru* wood plans with a 4x objective lens: transverse (a), longitudinal radial (b), and longitudinal tangential (c). Images in scanning electron microscopy: transverse (d), longitudinal radial (e), and longitudinal tangential (f).

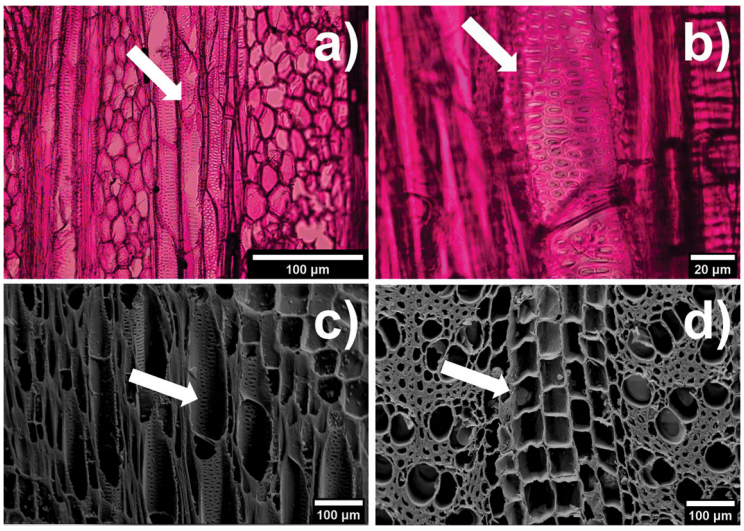


Figure 3: (a) Simple perforation plates, (b) Pits, (c) Scanning electron microscope of the pits, (d) Rays cells with deposit of substance inside.

The tangential arrangement (Figure 2c) shows a vessel frequency of 56.1/mm^2 and an average vessel diameter of 61.58 µm (Table 4). The vessel shape is spherical with tyloses, which can also be observed in Figure 4d. The obtained vessel frequency of 56.1/mm^2 can be considered high when compared with values reported in a prior study [42]. In that study, trees of nine eucalypt species (common hardwood in Brazil) were analyzed, and vessel frequencies between 9.2 and 14.7/mm^2 were measured. The high vessel frequency used in this research also explains the low density and high-water absorption capacity of the wood.

Simple perforated plates were identified (Figure 3a), and intervessel pits with alternating vessels running in the perpendicular direction were present (Figure 3b, 3c, 3b). The paratracheal axial parenchyma was present near the rays but only in extremely low quantities, and it was nonlignified (Figure 4a). *C. jamacaru* wood rays are exceptionally long and commonly visible to the naked eye (Figure 3d), and they are generally in the presence of radial canals (Figure 5b). They are multiseriate with a configuration of less than ten cells wide. Larger rays with a diameter of 156.85 µm and a frequency of 2.3/mm^2 (Table 3) were also observed. The rays are heterogeneous with almost circular cells in the regions adjacent to the rays and square cells in the center, representing the morphology of the rays. In this research, it was not possible to measure the ray length, as even an objective lens with an amplification of 1.25x were insufficient for observing whole ray. The large vessels, intervessel pits and simple perforated plates of *C. jamacaru* had large storage capacities (Figure 3). They show the ability to store

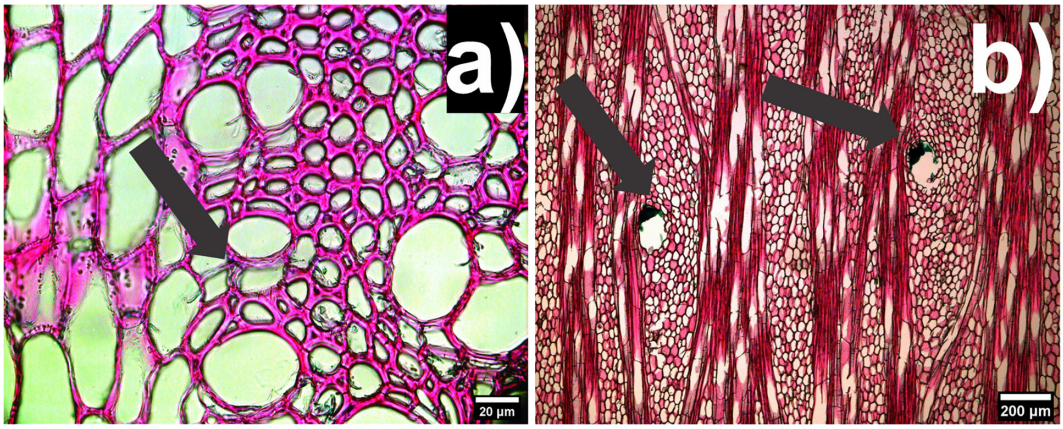


Figure 4: (a) The paratracheal axial parenchyma is present near rays, (b) radial canals of rays.

Table 4: *C. jamacaru* microscopic characteristics[1].

	RL (µm)	RF (no/mm²)	DV (µm)	VF (no/mm²)
Average	156.85	2.3	61.58	56.1
SD	39.41	0.48	9.54	8.97
VC	25.13%	21%	15.49%	15.99%

[1]Rays Larger (RL), Rays Frequency (RF), Diameter Vessel (DV), Vessels Frequency (FV), Standard Deviation (SD), Variation Coefficient (VC).

substances in the septate fibers and parenchyma, especially for rays that are large and long. It is very likely that this particular property allows them to adapt to the dry environments where the species is normally found [43].

3.3. Analysis of fibrous elements

The analysis of fibrous elements is important because these fibers are representative of the characteristics of the wood and, consequently, the technological application that can be given to it. In Figure 5, the *C. jamacaru* fibers (a, b, c) and vessel elements (a) can be seen at different levels of detail. The characterized results are given on Table 5.

According to SANTOS *et al*. [42], *C. jamacaru* fibers are short and can negatively influence the tensile strength and rupture strength. Thin cell walls, relative to the fiber diameter, can result in a low stiffness, low compressive strength, and low wood density, and they indicate a low cellulose content. The relationship between these parameters can be evaluated by the stiffness coefficient. For the *C. jamacaru* fibers, the average index was 23.2, which is slightly lower than the literature results where similar characterization works were done, other indices were 78.8 [16], 36.66 [11] and 65.26 [14].

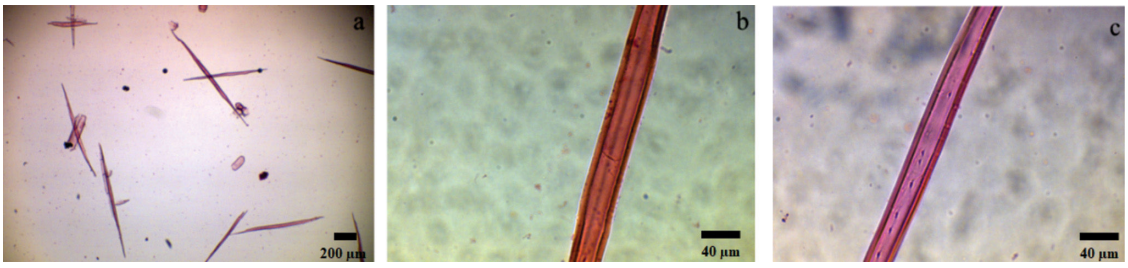


Figure 5: *C. jamacaru* fibers observed with a 4x objective lens (a) and 40x objective lens (b, c). In (b) we can see a septate fiber.

Table 5: Dimensional morphological analysis of *C. jamacaru* fibers (µm).

LENGTH	DIAMETER	LUMEN THICKNESS	CELL WALL THICKNESS
801.7 ± 206.5	34.6 ± 7.7	19.1 ± 7.2	7.8 ± 1.9

3.4. Chemical analyses

The results obtained through chemical analysis are shown in Table 6.

The chemical analyses indicated a remarkably high content of extractives compared to the average contents of hardwood and softwoods. This high content can be explained by the very low molecular weights of these components. Moreover, the results are also in good agreement with other indicators of low density [24]. The high content of extractives can also be a harmful factor for possible industrial applications, which implies the need for the pretreatment of the wood, for example, by washing in water to reduce the extractives, especially when they are used in cement-based composites [42, 44]. The cellulose content is low compared to the average content in hardwood and softwood, which is unfavorable, the amount of cellulose has a considerable influence on the physical and mechanical properties, elasticity and tensile strength of the fibers, which are important properties for structural applications. Hemicellulose could also be disadvantageous to properties such as hygroscopy, swelling and plasticity [45]. Finally, the lignin in the chemical structure is a natural component that reduces the susceptibility of wood to degradation. The high concentration of lignin in *C. jamacaru* can, therefore, lead to lower costs for treatments and/or products that help avoid this degradation [45].

3.5. Thermogravimetric analysis (TGA)

Thermogravimetric analysis results on *C. jamacaru* are shown in Figure 6 and represent the degradation of the wood microstructure as a function of temperature. It shows the weight loss curve that represents the disintegration of a given wood phase. The derivative curve (DTG) shows the characteristic peaks of mass reduction.

According to the literature, peaks that appear prior to 100°C are due to the evaporation of free water. Degradation of cellulose begins at temperatures of approximately 210°C, followed by a large endothermic reaction at 360°C. The depolymerization of hemicellulose should occur between 180 and 350°C, along with the degradation of lignin, which takes place between 250 and 500°C [46–48]. The measured TGA curves for

Table 6: *C. jamacaru,* chemical composition (in %).

	EXTRACTIVES	INSOLUBLE LIGNIN	CELLULOSE	HEMICELLULOSE	ASHES
Cactus	9.9 ± 0.7	26.7 ± 0.1	36.2 ± 2.8	25.3 ± 2.0	0.76 ± 0.1
Pinus[a]	6.0	31.5	41.0	10.5	0.4
Eucalyptus[a]	1.3	21.9	47.2	22	4.0

[a]Source: GARCÍA *et al*. [43].

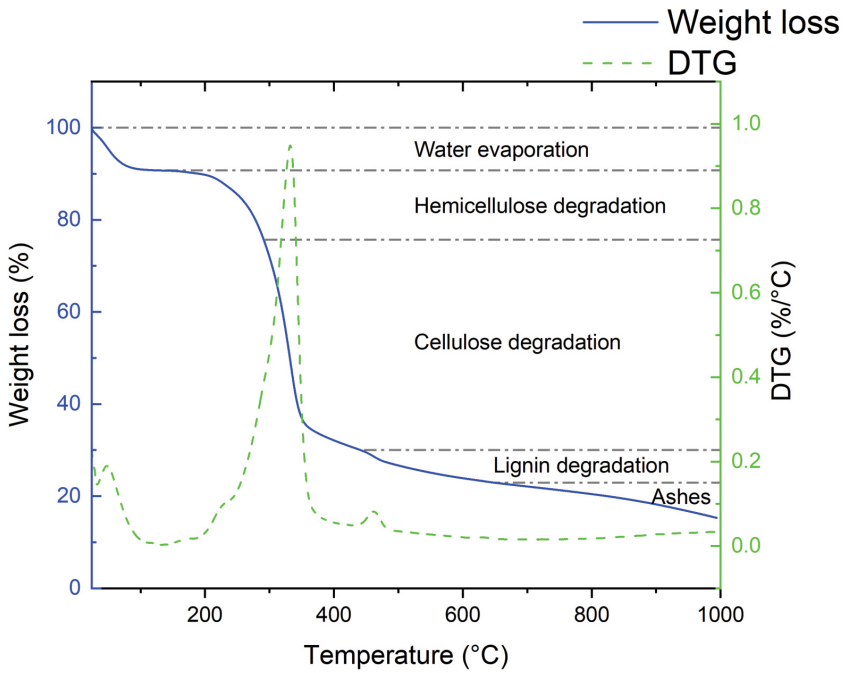


Figure 6: Thermogravimetric analysis of *C. jamacaru* wood.

C. jamacaru confirm this behavior, also indicating a large peak in the DTG curve around these temperatures. This peak, in fact, represents the overall behavior of several processes that run in parallel. In addition to this large peak, two smaller peaks were also observed at approximately 200–250°C and 400–450°C. According to the literature, these peaks are due to the initial degradation of hemicellulose and lignin. Carbon and inorganic components (ashes) remain at the end of the process (almost 16%).

3.6. FT-IR analysis of *C. jamacaru* wood

The FT-IR spectra of the *C. jamacaru* cactus wood shows a few characteristic peaks, such as at 1595 cm^{-1} and 1030 cm^{-1} (Figure 7). These peaks represent C = C stretching bonds, aromatic rings, and components such as flavonoids (components that make up tannins) and stretching = C-O-C =, oxo-aromatic components, respectively.

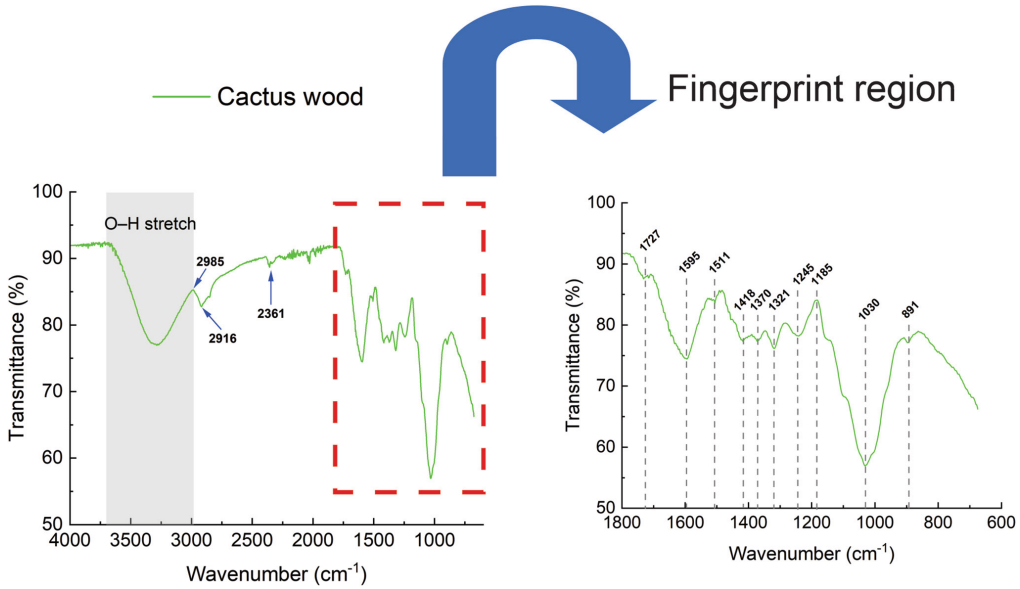


Figure 7: The FT-IR spectra of *C. jamacaru* cactus wood. Other peaks appearing on the graph of the *C. jamacaru* cactus wood represent carbon, oxygen, hydrogen, and nitrogen bonds. Other O-H bonds appear along the peaks in addition to carbon-carbon bonds and are known to be strong chemical bonds.

Table 7: FT-IR spectra of *C. jamacaru* cactus wood [18, 49–55].

FTIR BANDS ASSIGNMENT OF CACTUS WOOD AND PEAKS (cm^{-1})	
CACTUS WOOD	**BAND ASSIGNMENT**
3280	O–H stretch
2985	C–H stretching aromatic compounds
2916	C–H stretch. Aliphatics
2846	O–H stretch. Carboxylic acids
2361	N=C=O stretch
1727	C=O stretch. Carbonyl
1595	C=C stretch. Aromatics (6C) also flavonoids
1511	C=C–H stretch. Aromatic (in-plane) also furanics
1418	C–H deform. Aliph. C–C str. Ring B
1370	C–H bend. O–H bend (catechin)
1321	C–H bend. Aromatic conjugated sequences of polymer backbones
1245	O–H bend. in-plane deformation
1185	Phenyl acetates. C–O bending. C–H bend. Arom.
1030	Stretching =C–O–C=. Breathing oxo-aromatic compounds
891	C–H bend aromatic

The peaks in the FTIR pattern are also presented in Table 7. The band corresponding to the O-H bonding represented by the peak of 3280 cm^{-1} was well defined and represented the water present in the sample.

The two peaks at approximately 2920 and 2850 cm^{-1}, highlighted in Figure 7, are related to asymmetric and symmetric methyl and methylene stretching groups [46], which were attributed to the high amount of extractives present in this particular cactus wood (see also Table 6). According to POLETTO *et al.* [46], these observed sharp peaks in those regions can be explained by some compounds present in organic extractives, such as fatty acid methyl esters and/or phenolic acid methyl esters, which contain methyl and methylene groups.

3.7. Crystallography analyses of *C. jamacaru* fibers

X-ray diffraction (XRD) patterns of the *C. jamacaru* cactus fibers are shown in Figure 8. These patterns are typical for semicrystalline materials with an amorphous halo and crystalline peaks. The XRD patterns show a sharp peak near $2\theta = 22.6°$, which can be attributed to the (200) lattice plane of cellulose I. In Table 8, a crystalline fraction (CF) of 62.4% was calculated (Equation 4), using the deconvolution method, is different from the crystallinity index (CI) obtained by the Segal method (55.3%). According to a prior study [56], the Segal method has long been used because of its simplicity, but its results are controversial because it underestimates the amorphous fraction of cellulose. Additionally, a crystallite size of 2.37 nm was calculated with Scherrer's equation.

3.8. Raman analysis of mandacaru fibers

Figure 9 shows the Raman spectrum of cactus fibers. Raman spectroscopy is useful for identifying the chemical composition of lignocellulosic compounds and to rapidly characterize these materials [57, 58]. In this Raman spectrum, the band at 380 cm^{-1} is attributed to cellulose, and the band at 899 cm^{-1} corresponds to the in-plane symmetric stretching of C–O–C [59, 60]. The vibrational mode associated with (C–O–C) of the β - (1–4) glycosidic linkages of the glucopyranose units at 1120 cm^{-1} corresponding to symmetrical stretching encompasses both cellulose and hemicelluloses. The band at 1096 cm^{-1} is assigned to the asymmetric (C-O-C) stretching mode and is not influenced by noncellulosic carbohydrates [58]. The band at 1380 cm^{-1} is associated with CH_2 deformation vibrations, and the band at 1460 cm^{-1} is due to the CH_2 bending region [58, 59]. The peak at 1627 cm^{-1} may be due to phenyl groups of residual lignin that are normally identified in the region between 1600 and 1700 cm^{-1} [58, 59]. The strong band at 2891 cm^{-1} is due to the symmetric and asymmetric stretching vibrations of CH_2 [60].

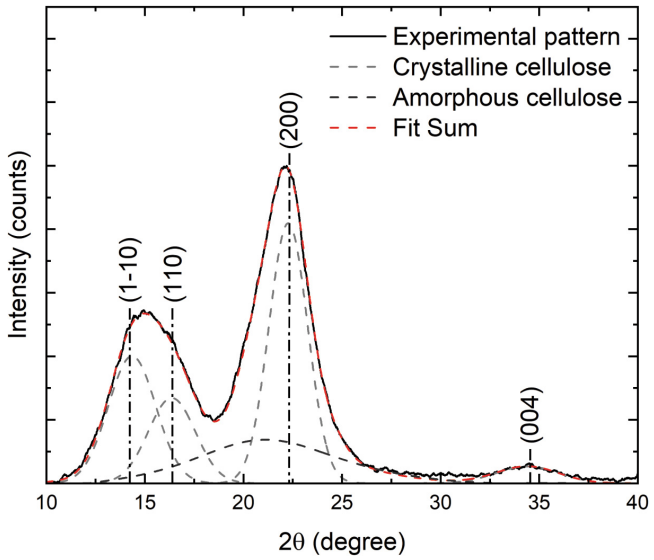


Figure 8: X-ray diffraction (XRD) of the *C. jamacaru* fibers.

Table 8: *C. jamacaru* fibers crystallography.

CRYSTALLINE FRACTION – CF (%)	SEGAL'S CRYSTALLINITY INDEX – CI (%)	CRYSTALLITE SIZE – CS (nm)
62.4	55.3	2.37

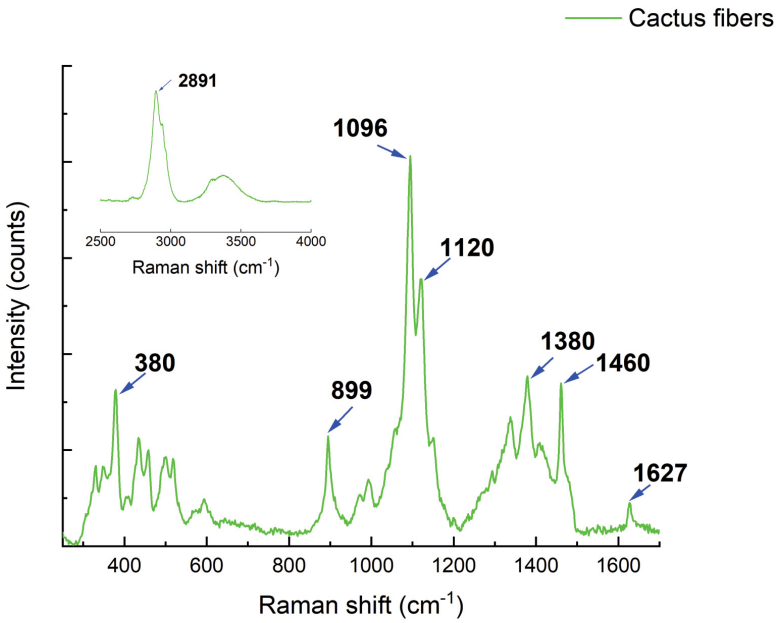


Figure 9: Raman spectra of *C. jamacaru* cactus fibers.

The cellulose crystallinity estimated by the Raman method (380 cm^{-1}) was 57.3%, similar to the value obtained by XRD analysis using the Segal method (55.3%).

3.9. Compressive Strength of *C. jamacaru* wood

Figure 10 provides the axial compressive strength results of *C. jamacaru* cactus wood. The corresponding data is shown in Table 9. The figure shows the results of five independent tests with an average maximum compressive strength of 38.2 MPa at a strain of 0.022 mm/mm. This value classifies the wood as a C_{30} strength class according to IPT [61].

Although the results show an impressive compressive strength, this wood has a low stiffness and a high deformation capacity. For a general C30 strength classification, a stiffness of approximately 14.5 GPa is expected. However, for the cactus wood used in this study, a stiffness of 2.31 GPa was calculated. This value

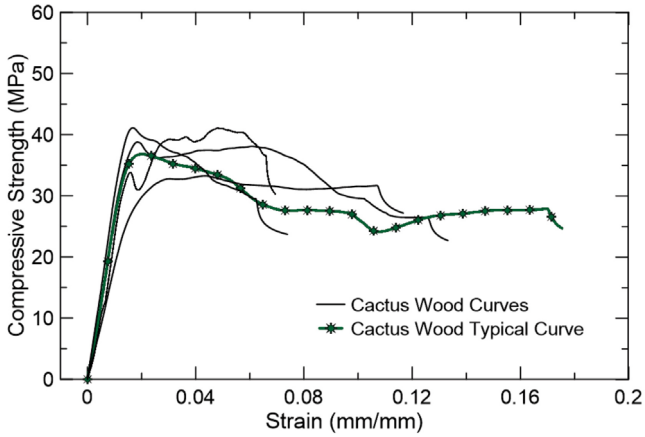


Figure 10: Axial compressive strength curves of *C. jamacaru* wood samples.

Table 9: Results of axial compressive strength tests of *C. jamacaru* wood.

SAMPLE	COMPRESSIVE STRENGTH (MPa)	STIFFNESS (GPa)	STRAIN AT PEAK LOAD (mm/mm)
Cactus Wood (*C. jamacaru*)	38.20 ± 2.94	2.3 ± 0.34	0.022 ± 0.001

is in good agreement with those of other cactus woods, such as Caixeta (*Simarouba amara Aubl.*), Cambará (*Erisma uncinatum Warm*), Quarubarana (*Eisma uncinatum*), Cedro Doce (*Cedrella spp.*) and Pinus bahamensis (*Pinus caribea var. bahamensis*), which have stiffnesses of 7.2, 10.4, 9.06, 8.05, and 7.1 GPa, respectively [61].

3.10. Bio-concrete

To date, the characterization of *C. jamacaru* cactus wood has revealed a robust morphological structure and chemical composition, with a density far below that of other types of hardwood. For this reason, its potential use as a lightweight bioaggregate in concrete was evaluated, making it a lightweight bio-concrete.

3.11. Fresh state properties

During mixing of the bio-concrete, no segregation occurred, and the bioaggregates were homogeneously distributed in the paste. Additionally, the adhesion between the bioaggregates and the paste turned out to be excellent. The mixture achieved good workability [38], as can be observed from the analyzed results in Table 10. The results show a good rheology, which is needed to promote a proper distribution of particles in the mix (see Figure 11a).

Due to the higher amount of compensation water (Table 2), the CBC200 mixture showed a higher spread than the CBC100 mix. However, these higher quantities of compensation water (200%) negatively influenced the compressive strength results. This could be avoided by applying presaturation of the bioaggregates in the mixing procedure.

3.12. Hardened state properties

The bio-concrete specimens containing *C. jamacaru* cactus wood and cement paste were demolded for one day, and the uniaxial compressive strength was evaluated after 28 days. The resulting stress versus strain curves are presented in Figure 11.

The maximum values for the compressive strength, modulus of elasticity and density of the bio-concretes are shown in Table 11.

Table 10: Flow table test (units in mm).

BLENDS	CBC100	CBC200
Consistency index	225	283

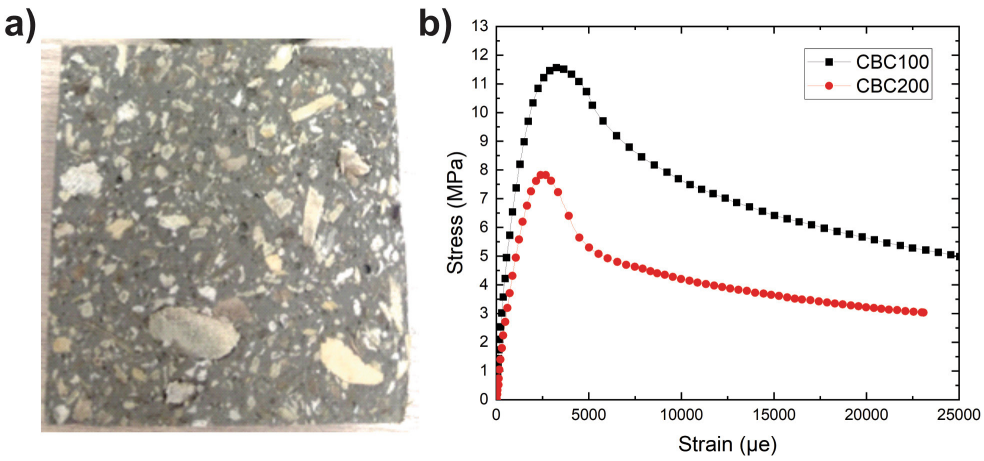


Figure 11: (a) Cross-section of a CBC100 bio-concrete, (b) Stress–strain curves for CBCs 100 and 200 representing the compressive strength of the bio-concretes.

Table 11: Physical and mechanical properties of the bio-concretes.

MIXTURE	COMPRESSIVE STRENGTH (MPa)	STRAIN (με)	E (GPa)	DENSITY (kg/m³)
CBC100	11.77 ± 1.04	24448.03 ± 3810.72	5.33 ± 0.25	1451.6
CBC200	8.18 ± 0.19	18337.4 ± 5122.4	4.47 ± 0.35	1284.0

The density of these bio-concretes ranged from 1284 to 1451.6 kg/m^3. According to RILEM [62] or DIN EN 206, they can be classified as lightweight materials since they have a density of less than 1800 kg/m^3 or 2000 kg/m^3, respectively. The density was mostly influenced by the amount of water and cactus wood (more water and more cactus wood resulted in lower densities).

From the stress versus strain curves, it could be observed that the bio-concretes show an initial elastic linear behavior, followed by a region of nonlinearity until the maximum tensile strength is reached. The rounded peak of the curve can be explained by microcracking and prerupture of the bio-concrete that allowed large deformations until failure.

Finally, it was observed that by reducing the compensating water by 50%, the density of both bio-concretes gained 11%, resulting in enhanced mechanical properties but lower workability.

4. CONCLUSIONS

From this work, the following conclusions can be drawn:

- The morphological and chemical characterization of cactus wood of the species *C. jamacaru* showed unique microstructural properties that are quite different from most common woods. The most plausible explanation for this is the adaptation of these woods to their natural habitat to survive in severe climate and poor soil conditions.
- The morphological structure of the cactus wood is very appropriate for absorbing water since it represents a fiber wall with medium thickness and a low spin index.
- Three washing cycles for extraction of the lignin phases from the cactus wood particles, combined with 3% calcium chloride, were effective for achieving proper cement hydration and hardening of the bio-concretes.
- Finally, two lightweight bio-concretes containing *C. jamacaru* bioaggregates embedded in a cement paste matrix were realized. Good physical, mechanical and workability properties were reached, and it turned out that *C. jamacaru* cactus wood can be a very appropriate alternative for bioaggregates in the production of bio-concretes for use in construction applications, in parts of the construction that do not directly involve a structural support.

5. ACKNOWLEDGMENTS

The authors would like to thank the Center of Analysis and Chemical Prospecting of the Federal University of Lavras for technical support involving all analyses and the NUMATS research center and LabEST of the Federal University of Rio de Janeiro. The authors also thank the Foundation for Research Support of Minas Gerais (FAPEMIG Grants No. TEC-AUC-00026-16, No. RED-00185-16, No. RED-00282-16, No. CEX-APQ-01865-17), the National Council for Scientific and Technological Development (CNPq Grants No. 310813/2017-4, No. 433027/2018-5, No. 433514/2018-3 and No. 204376/2018-1), the Agency for Financing Studies and Projects - FINEP (NANO No. 0501/16, and 02/2016), and CAPES (Finance Code 001) for financial and equipment support of this work. J.R-S. acknowledges support from the Pró-Reitoria de Pesquisa and Pró-Reitoria de Gestão (UFLA) and the prize L'ORÉAL-UNESCO-ABC Prêmio Para Mulheres na Ciência (Prize for Women in Science - Brazil/2017). The authors would like to thank the Laboratory of Electron Microscopy and Analysis of the Ultrastructural Federal University of Lavras (http://www.prp.ufla.br/labs/microscopia-eletronica/) and FINEP, FAPEMIG, CNPq and CAPES for supplying the equipment and technical support for experiments involving electron microscopy. And the FAPEMIG/CNPq project for young doctors BPD-00217-22 (Finance Code 150631/2023-5). Finally, the authors would like to thank the Institute of Construction and Building Materials of the TU Darmstadt in Germany for hosting Prof. Saulo Rocha Ferreira during his postdoctoral fellowship stay and for providing experimental support for this research.

6. BIBLIOGRAPHY

[1] FERREIRA, S.R., SILVA, F.A., LIMA, P.R.L., *et al*., "Effect of hornification on the structure, tensile behavior and fiber matrix bond of sisal, jute and curauá fiber cement based composite systems", *Construction & Building Materials*, v. 139, pp. 551–561, May. 2017. doi: http://doi.org/10.1016/j.conbuildmat.2016.10.004.

[2] MARANGON, G.P., FERREIRA, R.L.C., SILVA, J.A.A., *et al*., "Diametric distribution modeling of woody species in caatinga, semi-arid region of pernambuco state", *Ciência Florestal*, v. 26, n. 3, pp. 863–874, 2016. doi: http://doi.org/10.5902/1980509824214.

[3] DA GLORIA, M.Y.R., "*Desenvolvimento e caracterização de painéis sanduíches de concreto com núcleo leve e faces em laminados reforçados com fibras longas de sisal*", Tese de M.Sc., Universidade Federal do Rio de Janeiro, Rio de Janeiro, 2015.

[4] FERREIRA, S.R., SILVA, F.D.A., LIMA, P.R.L., *et al*., "Effect of fiber treatments on the sisal fiber properties and fiber-matrix bond in cement based systems", *Construction & Building Materials*, v. 101, pp. 730–740, 2015. doi: http://doi.org/10.1016/j.conbuildmat.2015.10.120.

[5] NEVES JUNIOR, A., FERREIRA, S.R., TOLEDO FILHO, R.D., *et al*., "Effect of early age curing carbonation on the mechanical properties and durability of high initial strength Portland cement and lime-pozolan composites reinforced with long sisal fibres", *Composites. Part B, Engineering*, v. 163, pp. 351–362, Apr. 2019. doi: http://doi.org/10.1016/j.compositesb.2018.11.006.

[6] FRAZÃO, C., BARROS, J., TOLEDO FILHO, R., *et al*., "Development of sandwich panels combining sisal fiber-cement composites and fiber-reinforced lightweight concrete", *Cement and Concrete Composites*, v. 86, pp. 206–223, 2018. doi: http://doi.org/10.1016/j.cemconcomp.2017.11.008.

[7] SALES, M.S.L., MARTINS, L.V., SOUZA, I., *et al*., "*Cereus jamacaru* de Candolle (Cactaceae), o Mandacaru do nordeste brasileiro", *Publicatio UEPG. Ciências Biológicas e da Saúde*, v. 20, n. 2, pp. 135–142, 2014. doi: http://doi.org/10.5212/Publ.Biologicas.v.20i2.0006.

[8] EDWARD, A., *The cactus family*, Portland, Timbre Press, 2001.

[9] LORENZI, H., *Árvores brasileiras: manual de identificação e cultivo de plantas arbóreas do Brasil*, 2 ed., Nova Odessa, Instituto Plantarum, 2016.

[10] NEPOMUCENO, N.C., SANTOS, A.S.F., OLIVEIRA, J.E., *et al*., "Extraction and characterization of cellulose nanowhiskers from Mandacaru (*Cereus jamacaru* DC.) spines", *Cellulose*, v. 24, n. 1, pp. 119–129, Jan. 2017. doi: http://doi.org/10.1007/s10570-016-1109-5.

[11] BEVILAQUA, M.R.R., SANTANA FILHO, A.P., MANGOLIN, C.A., *et al*., "Genetic and chemical diversity in seeds of cactus mandacaru (*Cereus* sp.) from two edaphoclimatic regions contrasting", *Anais da Academia Brasileira de Ciências*, v. 87, n. 2, pp. 765–776, Jun. 2015. doi: http://doi.org/10.1590/0001-3765201520140029.

[12] ŘEZANKA, T., DEMBITSKY, V.M., "Very-long-chain alkyl esters in *Cereus peruvianus* wax", *Phytochemistry*, v. 47, n. 6, pp. 1145–1148, Mar. 1998. doi: http://doi.org/10.1016/S0031-9422(97)00668-7.

[13] OLIVEIRA, A.J.B., MACHADO, M.F., "Alkaloid production by callous tissue cultures of Cereus peruvianus (Cactaceae)", *Applied Biochemistry and Biotechnology*, v. 104, n. 2, pp. 149–155, 2003. doi: http://doi.org/10.1385/ABAB:104:2:149. PubMed PMID: 12603103.

[14] ALVAREZ, M., COSTA, S.C., UTUMI, H., *et al*., "The anionic glycan from the cactus cereus peruvianus", *Applied Biochemistry and Biotechnology*, v. 34–35, n. 1, pp. 283–295, Mar. 1992. doi: http://doi.org/10.1007/BF02920552.

[15] GÓMEZ-GALERA, S., PELACHO, A.M., GENÉ, A., *et al*., "The genetic manipulation of medicinal and aromatic plants", *Plant Cell Reports*, v. 26, n. 10, pp. 1689–1715, Sep. 2007. doi: http://doi.org/10.1007/s00299-007-0384-x. PubMed PMID: 17609957.

[16] CÁRDENAS, R., ARGUELLES, M., GOYCOOLEA, M., "On the possible role of opuntia ficus-indica mucilage in lime mortar performance in the protection of historical buildings", *Journal of the Professional Association for Cactus Development*, v. 3, pp. 64–71, 1998.

[17] TORRES-ACOSTA, A.A., "Opuntia-Ficus-Indica (Nopal) mucilage as a steel corrosion inhibitor in alkaline media", *Journal of Applied Electrochemistry*, v. 37, n. 7, pp. 835–841, Jun. 2007. doi: http://doi.org/10.1007/s10800-007-9319-z.

[18] RAMPAZZI, L., COLOMBINI, M.P., CONTI, C., *et al*., "Technology of medieval mortars: an investigation into the use of organic additives", *Archaeometry*, v. 58, n. 1, pp. 115–130, Feb. 2016. doi: http://doi.org/10.1111/arcm.12155.

[19] INTERNATIONAL AVIATION WOMENS ASSOCIATION, *IAWA list of microscopic features for hardwood identification*, Leesburg, IAWA, v. 3, pp. 219–332, 1988.

[20] FRANKLIN, G.L., "Preparation of thin sections of synthetic resins and wood-resin composites, and a new macerating method for wood", *Nature*, v. 155, n. 3924, pp. 5, 1945. doi: http://doi.org/10.1038/155051a0.

[21] INSTITUTO DE PESQUISAS TECNOLÓGICAS, *Madeira: o que é e como pode ser processada e utilizada* (Boletim ABPM 36), São Paulo, IPT, 1985.

[22] CLARKE, C., GARBUTT, D.C.F., PEARCE, J., "Growth and wood properties of provenances and trees of nine eucalypt species", *Appita Journal*, v. 50, n. 2, pp. 121–130, 1997.

[23] VILLASEÑOR ARAIZA, J.C., RUTIAGA QUIÑONES, J.G., "La madera de *Casuarina equisetifolia* L., química e índices de calidad de pulpa", *Madera y Bosques*, v. 6, n. 1, pp. 29–40, Sep. 2016. doi: http://doi.org/10.21829/myb.2000.611340.

[24] COLLI, A., VITAL, B.R., CARNEIRO, A.C.O., *et al*., "Propriedades de chapas fabricadas com partículas de madeira de paricá (*Schyzolobium amazonicum* Huber ex. Ducke) e fibras de coco (*Cocos nucifera* L.)", *Revista Árvore*, v. 34, n. 2, pp. 333–338, Apr. 2010. doi: http://doi.org/10.1590/S0100-67622010000200016.

[25] BORJA DE LA ROSA, A., MACHUCA, R., FUENTES SALINAS, M., *et al*., "Caracterización tecnológica de la madera de *Juniperus flaccida* var. *poblana* Martínez", *Revista Chapingo Serie Ciencias Forestales y del Ambiente*, v. XVI, n. 2, pp. 261–280, Dec. 2010. doi: http://doi.org/10.5154/r.rchscfa.2010.09.083.

[26] BROWNING, B.L., *The chemistry of wood*, Warrenvile, Interscience, 1963.

[27] KENNEDY, J.F., *Wood and cellulosics: Industrial utilisation, biotechnology, structure, and properties*, Chichester, Halsted Press, 1987.

[28] NISHIYAMA, Y., LANGAN, P., CHANZY, H., "Crystal structure and hydrogen-bonding system in cellulose Iβ from synchrotron X-ray and neutron fiber diffraction", *Journal of the American Chemical Society*, v. 124, n. 31, pp. 9074–9082, Aug. 2002. doi: http://doi.org/10.1021/ja0257319. PubMed PMID: 12149011.

[29] FRENCH, A.D., "Increment in evolution of cellulose crystallinity analysis", *Cellulose*, v. 27, n. 10, pp. 5445–5448, 2020. doi: http://doi.org/10.1007/s10570-020-03172-z.

[30] SEGAL, L., CREELY, J.J., MARTIN JUNIOR, A.E., *et al*., "An empirical method for estimating the degree of crystallinity of native cellulose using the X-ray diffractometer", *Textile Research Journal*, v. 29, n. 10, pp. 786–794, 1959. doi: http://doi.org/10.1177/004051755902901003.

[31] LANGFORD, J.I., WILSON, A.J.C., "Scherrer after sixty years: a survey and some new results in the determination of crystallite size", *Journal of Applied Crystallography*, v. 11, n. 2, pp. 102–113, 1978. doi: http://doi.org/10.1107/S0021889878012844.

[32] AGARWAL, U.P., REINER, R.S., RALPH, S.A., "Cellulose I crystallinity determination using FT-Raman spectroscopy: univariate and multivariate methods", *Cellulose*, v. 17, n. 4, pp. 721–733, 2010. doi: http://doi.org/10.1007/s10570-010-9420-z.

[33] EL-ABASSY, R.M., DONFACK, P., MATERNY, A., "Discrimination between Arabica and Robusta green coffee using visible micro Raman spectroscopy and chemometric analysis", *Food Chemistry*, v. 126, n. 3, pp. 1443–1448, Jun. 2011. doi: http://doi.org/10.1016/j.foodchem.2010.11.132.

[34] BAŽANT, Z.P., "Size effect", *International Journal of Solids and Structures*, v. 37, n. 1–2, pp. 69–80, Jan. 2000. doi: http://doi.org/10.1016/S0020-7683(99)00077-3.

[35] BUYUKSARI, U., AS, N., DUNDAR, T., *et al*., "Micro-mechanical properties of oak wood and comparison with standard-sized samples", *Maderas. Ciencia y Tecnología*, v. 19, n. 4, pp. 481–494, 2017. doi: http://doi.org/10.4067/S0718-221X2017005000801.

[36] SCHLOTZHAUER, P., NELIS, P.A., BOLLMUS, S., *et al*., "Effect of size and geometry on strength values and MOE of selected hardwood species", *Wood Material Science & Engineering*, v. 12, n. 3, pp. 149–157, May. 2017. doi: http://doi.org/10.1080/17480272.2015.1073175.

[37] AMERICAN SOCIETY FOR TESTING AND MATERIALS, *ASTM D2395-17 Standard Test Methods for Density and Specific Gravity (Relative Density) of Wood and Wood-Based Materials*, West Conshohocken, ASTM International, 2017.

[38] ANDREOLA, V.M., DA GLORIA, M.Y.R., TOLEDO FILHO, R.D., "Desenvolvimento de biocompósitos contendo partículas de bambu", In: *Anais do II Congresso Luso-Brasileiro de Materiais de Construção Sustentáveis*, João Pessoa, 2016.

[39] SANTOS, D., DA GLORIA, M., ANDREOLA, V., *et al*., "Compressive stress strain behavior of workable bio-concretes produced using bamboo, rice husk and wood shavings particles", *Academic Journal of Civil Engineering*, v. 35, n. 2, pp. 211–217, 2017.

[40] BÜYÜKSARI, Ü., AS, N., DÜNDAR, T., *et al*., "Comparison of micro- and standard-size specimens in evaluating the flexural properties of scots pine wood", *BioResources*, v. 11, n. 4, Nov. 2016. doi: http://doi.org/10.15376/biores.11.4.10540-10548.

[41] AMERICAN SOCIETY FOR TESTING AND MATERIALS, *ASTM C39/C39M-18 Standard Test Method for Compressive Strength of Cylindrical Concrete Specimens*, West Conshohocken, ASTM International, 2018.

[42] SANTOS, D.O.J., GLORIA, M.Y.R., ANDREOLA, V.M., *et al*., "Compressive stress strain behavior of workable bio-concretes produced using bamboo, rice husk and wood shavings particles", In: *Proceedings of the 2nd International Conference on Bio-Based Building Materials, RILEM*, pp. 211–217, June 2017.

[43] GARCÍA, A., GONZÁLEZ ALRIOLS, M., LABIDI, J., "Evaluation of different lignocellulosic raw materials as potential alternative feedstocks in biorefinery processes", *Industrial Crops and Products*, v. 53, pp. 102–110, Feb. 2014. doi: http://doi.org/10.1016/j.indcrop.2013.12.019.

[44] SONSIN, J.O., GASSON, P.E., BARROS, C.F., *et al*., "A comparison of the wood anatomy of 11 species from two cerrado habitats (cerrado *s.s.* and adjacent gallery forest)", *Botanical Journal of the Linnean Society*, v. 170, n. 2, pp. 257–276, 2012. doi: http://doi.org/10.1111/j.1095-8339.2012.01282.x.

[45] FERREIRA, S.R., PEPE, M., MARTINELLI, E., *et al*., "Influence of natural fibers characteristics on the interface mechanics with cement based matrices", *Composites. Part B, Engineering*, v. 140, pp. 183–196, 2018. doi: http://doi.org/10.1016/j.compositesb.2017.12.016.

[46] POLETTO, M., ZATTERA, A.J., SANTANA, R.M.C., "Structural differences between wood species: Evidence from chemical composition, FTIR spectroscopy, and thermogravimetric analysis", *Journal of Applied Polymer Science*, v. 126, n. S1, pp. E337–E344, Oct. 2012. doi: http://doi.org/10.1002/app.36991.

[47] MELO FILHO, J.A., SILVA, F.A., TOLEDO FILHO, R.D., "Degradation kinetics and aging mechanisms on sisal fiber cement composite systems", *Cement and Concrete Composites*, v. 40, pp. 30–39, Jul. 2013. doi: http://doi.org/10.1016/j.cemconcomp.2013.04.003.

[48] MARTIN, A.R., MARTINS, M.A., SILVA, O.R.R.F., *et al*., "Studies on the thermal properties of sisal fiber and its constituents", *Thermochimica Acta*, v. 506, n. 1–2, pp. 14–19, Jul. 2010. doi: http://doi.org/10.1016/j.tca.2010.04.008.

[49] AJUONG, E.-M.A., BIRKINSHAW, C., "The effects of acetylation on the extractives of Sitka Spruce (*Picea sitchensis*) and Larch (*Larix leptoleptis*) wood", *Holz als Roh- und Werkstoff*, v. 62, n. 3, pp. 189–196, Jun. 2004. doi: http://doi.org/10.1007/s00107-004-0481-2.

[50] BURKET, C.L., RAJAGOPALAN, R., MARENCIC, A.P., *et al*., "Genesis of porosity in polyfurfuryl alcohol derived nanoporous carbon", *Carbon*, v. 44, n. 14, pp. 2957–2963, Nov. 2006. doi: http://doi.org/10.1016/j.carbon.2006.05.029.

[51] CHOURA, M., BELGACEM, N.M., GANDINI, A., "Acid-catalyzed polycondensation of furfuryl alcohol: mechanisms of chromophore formation and cross-linking", *Macromolecules*, v. 29, n. 11, pp. 3839–3850, Jan. 1996. doi: http://doi.org/10.1021/ma951522f.

[52] OO, C.W., KASSIM, M.J., PIZZI, A., "Characterization and performance of *Rhizophora apiculata* mangrove polyflavonoid tannins in the adsorption of copper (II) and lead (II)", *Industrial Crops and Products*, v. 30, n. 1, pp. 152–161, Jul. 2009. doi: http://doi.org/10.1016/j.indcrop.2009.03.002.

[53] SONG, C., WANG, T., WANG, X., *et al*., "Preparation and gas separation properties of poly(furfuryl alcohol)-based C/CMS composite membranes", *Separation and Purification Technology*, v. 58, n. 3, pp. 412–418, Jan. 2008. doi: http://doi.org/10.1016/j.seppur.2007.05.019.

[54] TONDI, G., PETUTSCHNIGG, A., "Middle infrared (ATR FT-MIR) characterization of industrial tannin extracts", *Industrial Crops and Products*, v. 65, pp. 422–428, Mar. 2015. doi: http://doi.org/10.1016/j.indcrop.2014.11.005.

[55] UNSALAN, O., ERDOGDU, Y., GULLUOGLU, M.T., "FT-Raman and FT-IR spectral and quantum chemical studies on some flavonoid derivatives: Baicalein and Naringenin", *Journal of Raman Spectroscopy*, v. 40, n. 5, pp. 562–570, May. 2009. doi: http://doi.org/10.1002/jrs.2166.

[56] FRENCH, A.D., "Idealized powder diffraction patterns for cellulose polymorphs", *Cellulose*, v. 21, n. 2, pp. 885–896, 2014. doi: http://doi.org/10.1007/s10570-013-0030-4.

[57] AGARWAL, U.P., RALPH, S.A., "FT-Raman spectroscopy of wood: identifying contributions of lignin and carbohydrate polymers in the spectrum of black spruce (*Picea mariana*)", *Applied Spectroscopy*, v. 51, n. 11, pp. 1648–1655, Nov. 1997. doi: http://doi.org/10.1366/0003702971939316.

[58] BESBES, I., VILAR, M.R., BOUFI, S., "Nanofibrillated cellulose from Alfa, Eucalyptus and Pine fibres: preparation, characteristics and reinforcing potential", *Carbohydrate Polymers*, v. 86, n. 3, pp. 1198–1206, 2011. doi: http://doi.org/10.1016/j.carbpol.2011.06.015.

(cc) BY

[59] YANG, C., CHEN, C., PAN, Y., *et al*., "Flexible highly specific capacitance aerogel electrodes based on cellulose nanofibers, carbon nanotubes and polyaniline", *Electrochimica Acta*, v. 182, pp. 264–271, 2015. doi: http://doi.org/10.1016/j.electacta.2015.09.096.

[60] AGARWAL, U.P., *Raman spectroscopy in the analysis of cellulose nanomaterials*, Washington, D.C., American Chemical Society, pp. 75–90, 2017. doi: http://doi.org/10.1021/bk-2017-1251.ch004.

[61] INSTITUTO DE PESQUISAS TECNOLÓGICAS, *Informações sobre madeiras*, São Paulo, IPT, 2018.

[62] RILEM, *Classification fonctionnelle des bétons légers* [Functional classification of lightweight concrete], Champs-sur-Marne, 1972.